Structure and chemical durability of lead crystal glass

Frederic Angeli, Patrick Jollivet, Thibault Charpentier, Maxime Fournier, S. Gin

Environmental Science & Technology

Article

pubs.acs.org/est

Structure and Chemical Durability of Lead Crystal Glass

Frédéric Angeli,*[,†] Patrick Jollivet,[†] Thibault Charpentier,[‡] Maxime Fournier,[†] and Stéphane Gin[†]

[†]CEA, DEN, DTCD, SECM, F-30207 Bagnols-sur-Cèze, France

[‡]NIMBE, CEA, CNRS, Université Paris-Saclay CEA Saclay, F-91191 Gif-sur-Yvette, France

Supporting Information

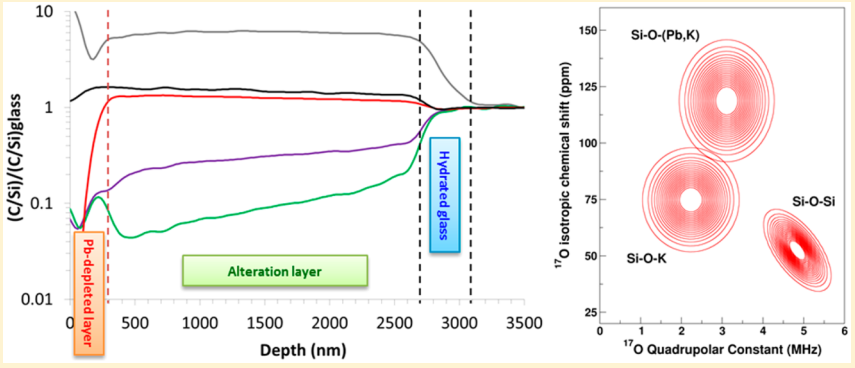

ABSTRACT: Silicate glasses containing lead, also called lead crystal glasses, are commonly used as food product containers, in particular for alcoholic beverages. Lead's health hazards require major attention, which can first be investigated through the understanding of Pb release mechanisms in solution. The behavior of a commercial crystal glass containing 10.6 mol % of PbO (28.3 wt %) was studied in a reference solution of 4% acetic acid at 22, 40, and 70 °C at early and advanced stages of reaction. High-resolution solid-state ^{17}O and ^{29}Si NMR was used to probe the local structure of the pristine and, for the first time, of the altered lead crystal glass. Inserted into the vitreous structure between the network formers as Si−O−Pb bonds, Pb does not form Pb−O−Pb clusters which are expected to be more easily leached. A part of K is located near Pb, forming mixed Si−O−(Pb,K) near the nonbridging oxygens. Pb is always released into the solution following a diffusion-controlled dissolution over various periods of time, at a rate between 1 and 2 orders of magnitude lower than the alkalis (K and Na). The preferential release of alkalis is followed by an *in situ* repolymerization of the silicate network. Pb is only depleted in the outermost part of the alteration layer. In the remaining part, it stays mainly surrounded by Si in a stable structural configuration similar to that of the pristine glass. A simple model is proposed to estimate the Pb concentration as a function of glass surface, solution volume, temperature, and contact time.

I. INTRODUCTION

For thousands of years, lead has been used in the preparation of silicate glasses, in particular because it enables the temperature range of the glass-forming ability to be extended. It was widely used not only in various archeological artifacts, such as enamels and glazes,[1] but also in applications for optics, electronics,[2] or even in protection against irradiation.[3] Since the 17th century, lead oxide has been added to alkali silicate to form a material called lead crystal, giving a high clarity and a characteristic sonority. Lead crystal has been regulated since 1969 in order to guarantee the quality of the material, based on density, refraction index, and lead content criteria. Lead oxide must be at least 24 wt % to be designated as crystal.

Exposure to Pb is hazardous for the environment and for human health when it accumulates in the organism.[4,5] It is therefore of primary importance to understand the behavior of this element in manufactured articles throughout their conditions of use, particularly if they contain liquids intended for human consumption.

Numerous empirical studies have been carried out to examine the Pb leaching from glass or from glass ceramic in reactive environments, particularly in contact with different actual beverages or simple synthetic solutions such as acetic or nitric acid.[6−20] In commercial lead crystal glasses, it has generally been observed that the release of alkalis and Pb ions exhibited a square root time dependence through a diffusion process.[11,15,17,18] Their leaching kinetics usually increase with the temperature and with the acetic acid concentration.[17] During successive contacts, a decrease in the release of Pb has been observed with each additional solution contact.[16] However, there is a lack of mechanistic understanding able to account for and predict the Pb behavior, in relation with its structural evolution during leaching.

Received: June 24, 2016
Revised: October 4, 2016
Accepted: October 10, 2016
Published: October 10, 2016

DOI: 10.1021/acs.est.6b02971
Environ. Sci. Technol. 2016, 50, 11549−11558

The structural arrangements coming from the incorporation of Pb into a silicate network can significantly modify glass macroscopic properties, in particular its chemical durability.[10] For a low content, typically under 40 mol % of PbO, a major part of Pb may be assimilated to a modifier cation,[21] thus resembling an alkaline-earth type cation, forming ionic bonds with nonbridging oxygens (NBOs).[22] When a large amount of Pb is added to reach an orthosilicate composition (Pb/Si = 2), oxygens are then linked to the metallic cations to form metal-bridging oxygen bonds Pb−O−Pb.[23−25] Pb is then associated in trigonal pyramids connected by their edges to form interlinked Pb_2O_4 units.[26] In this case, Pb mainly takes a network former configuration, forming more covalent bonds with the oxygens.[21,27,28] For contents greater than ∼60 mol % of PbO, Pb forms its own vitreous network.[29] Pb has the special feature of having the ability to form a glass in a very wide range of concentrations,[30] up to more than 80 mol % of PbO for a rapidly quenched material.[23,29] When Pb acts as a network former cation, unlike most network formers, it does not provide to the glass a greater chemical durability: Pb clusters form extended lead-rich domains which are rapidly leached. There are percolation pathways between these domains, and the Pb release into solution strongly increases.[10] Generally, whatever the solution pH, the release of Pb seems to decrease when its content is lower.[10,19,31]

The mechanisms of aqueous alteration of lead crystal glasses compared to their structural evolution during leaching had not been approached prior to this study. In order to give new insights into the understanding of Pb leaching of industrial glasses, a structural approach for the glass as well as its alteration layer was applied in this work, together with the evolution of the elemental alteration profiles. Combined with the solution analyses under various experimental conditions, it enabled the mechanisms involved to be better defined.

This paper is focused on a commercial lead crystal glass containing 10.6 mol % of PbO (28.3 wt %). Complementary experiments, which enabled various kinetics regimes to be reached, are conducted to simulate the short- and long-term behavior of the crystal glass. Hydrolysis mechanisms were specifically investigated using dynamic experiments with high flow rate, whereas interdiffusion mechanisms were highlighted from static experiments using saturated solutions with respect to amorphous silica (avoiding hydrolysis mechanisms[32]). The experiments were carried out in 4% (*v*/*v*) acetic acid solution, which is commonly used as a standard reference solution.[13,17,33] The local structure of pristine and altered materials was characterized by high-resolution solid-state Nuclear Magnetic Resonance (NMR) of silicon-29 and oxygen-17. Elemental depth profiling were monitored by Time-of-Flight Secondary Ion Mass Spectrometry (ToF-SIMS).

II. EXPERIMENTAL SECTION

Materials. Two glasses were used for this study, the first being a commercial glass with the molar composition $77.1SiO_2 - 0.8Na_2O - 11.3K_2O - 10.6PbO - 0.2Sb_2O_3$. The glass chemical composition was checked by Inductively Coupled Plasma-Optical Emission Spectroscopy (ICP-OES) analysis after acidic dissolution (HCl+HNO_3+HF). The analysis gave the theoretical composition at less than 1% of nominal composition. A second glass was synthesized to be enriched in oxygen-17 (without Sb addition). 200 mg of glass was prepared by sol−gel from a mixture of alkoxides hydrolyzed by 90% enriched water in ^{17}O.[34] After reaction, this mixture was maintained at 1270 °C for 30 min under argon atmosphere in a Pt/Au crucible. ICP-OES analysis gave the molar composition: $80.7SiO_2 - 0.7Na_2O - 10.8K_2O - 7.9PbO$.

NMR. ^{29}Si MAS NMR data were collected on a Bruker 300WB Avance I spectrometer operating at a magnetic field of 7.02 T (I = 1/2, Larmor frequency ν_0 = 59.4 MHz). A Bruker 4 mm (outer diameter of the rotor) CPMAS Probe was used at a spinning frequency of 10 kHz. Silicon spectra were acquired using the CPMG sequence,[35] by typically accumulating 32 echoes with an echo delay of 4 ms between consecutive 180° pulses. The echoes were then summed up and Fourier transformed to obtain the spectra. A 20 s recycling time was used; checks were carried out that no spectral deformation was observed for longer recycling delays (up to 1200 s). The spectra were referenced to an external tetrakis(trimethylsilyl)silane (TKS) sample, for which the highest intensity peak was positioned at −9.9 ppm from that of TMS.

^{17}O MAS NMR data were collected on a Bruker 500WB Avance II spectrometer operating at a magnetic field of 11.72 T (I = 5/2, Larmor frequency ν_0 = 67.67 MHz). A Bruker 4 mm CPMAS probe was used at a spinning frequency of 12.5 kHz. MAS NMR spectra were acquired using a rotor synchronized Hahn echo pulse sequence to minimize the baseline distortion, with soft 90° and 180° pulses (selective on the central transition, RF field 25 kHz), an echo delay of one rotation period, and a recycle delay of 1 s (no change in line shape was observed for longer delay). The MQMAS spectra were acquired with 64 t_1 rotor-synchronized increments (of one rotation period) in the first dimension and a 1 s repetition time (4500 FIDs per t_1 value were collected). The Z-filter pulse sequence[36] was used with first and second pulse durations of 5 and 2 μs, respectively (RF field 60 kHz), and a third 90° soft pulse, selective on the central transition, of 3.5 μs (RF field 25 kHz).[37] ^{17}O reported NMR parameters were obtained from the fitting of NMR parameter distributions (modeled as the product of three Gaussian distributions, one for each parameter, namely the isotropic chemical shift δ_{iso}, the quadrupolar coupling constant C_Q, and the asymmetry parameter η) to the MAS and MQMAS NMR parameters, as was detailed in refs 34 and 38. The spectra were referenced to an external $H_2{}^{17}O$ solution.

^1H and $^1H-^{17}O$ Cross-Polarization experiments were performed in order to better define the NMR parameters of the small Si−OH peaks observed in the altered glass. Some experiments are detailed in the Supporting Information. All data were processed and fitted using an in-house written software.[38]

ToF-SIMS. Depth profiles were analyzed by ToF-SIMS (IONTOF TOF 5) using O_2^+ sputtering beams analyzing a surface area of 60 × 60 μm^2. Oxygen beam was tuned at 2 kV, 500 nA. Elemental profiles were normalized to that of Si to avoid matrix effects. The depth of the craters was measured after the analyses, and profiles were calculated assuming that the sputtering rate was constant.

Leaching Experiments. After crushing and sieving, the selected size fractions (20−40 and 63−125 μm) were washed by decantation in acetone to remove fine particles, according to Stokes' law. Then, the specific surface areas of the glass powders were measured by krypton physical adsorption on the sample surface with the BET method on a Micromeritics ASAP 2020.

Forward dissolution rate r_0 was measured using a single-pass flow-through test (SPFT) at 22, 40, and 70 °C. About 100 mg of glass powder (63−125 μm particle size fraction) was placed

DOI: 10.1021/acs.est.6b02971
Environ. Sci. Technol. 2016, 50, 11549−11558

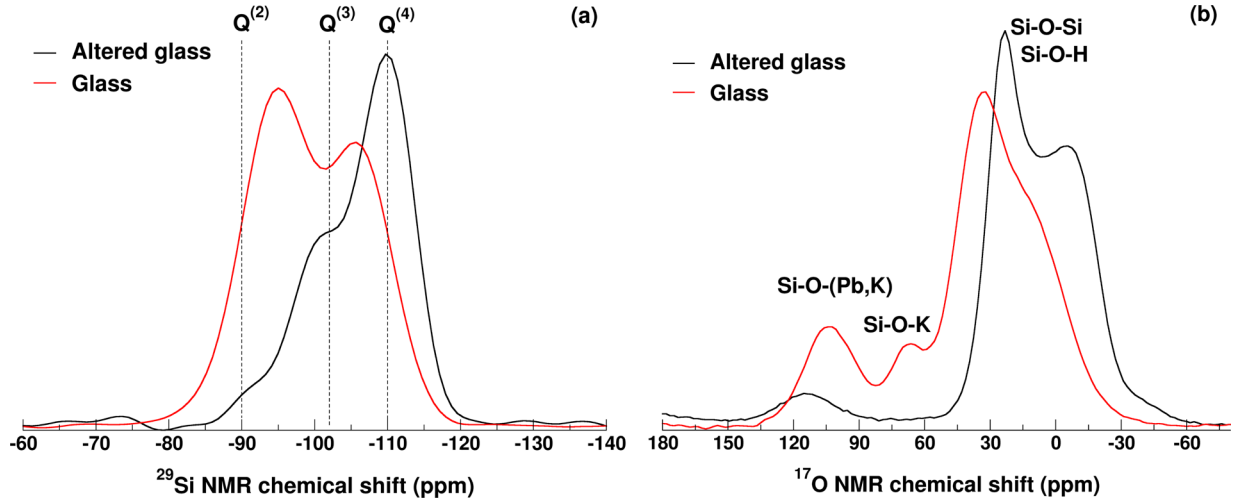

Figure 1. (a) ^{29}Si MAS NMR (Q^n species are identified by broken lines for the altered glass, their positions are slightly shifted between pristine and altered glass) and (b) ^{17}O MAS NMR spectra of pristine and altered glass after 35 days at 70 °C in acetic acid solution with oxygen-17 enriched water.

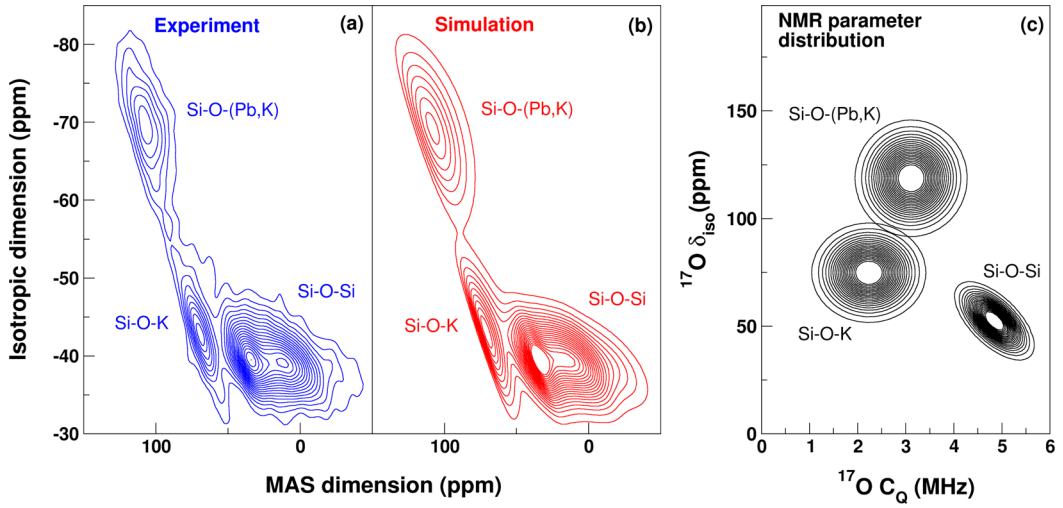

Figure 2. Contour plots of the experimental (a) and simulated (b) ^{17}O MQMAS NMR spectra and (c) the two-dimensional projection of the extracted ^{17}O NMR parameter distribution (δ_{iso} and C_Q).

into a column made of PTFE, through which 4% (v/v) acetic acid was passed at a flow rate between 0.2 and 0.6 mL·min^{-1} to avoid any feedback effect on the rate by glass constituent elements released into solution. The temperature of the leaching solution was monitored continuously at the reactor inlet, and a maximum variation of ±1 °C was allowed. The leachate was regularly sampled, and the Si concentration was determined photometrically with a Merck Spectroquant test and a Cary Varian UV−visible spectrophotometer with a method analogous to ASTM D859-10. Other elements were analyzed by ICP-OES (Thermo Scientific ICAP 3600 DUO). The equivalent thicknesses of altered glass, Eth_i (m), were calculated with the eq 1

$$Eth_i(t) = \frac{1}{\rho}\sum_{j=1}^{j=n}\frac{1}{x_i \times SSA \times m}\left[\frac{(C(i)_j + C(i)_{j+1})}{2} \times Q \times (t_{j+1} - t_j)\right] \quad (1)$$

where ρ is the glass density (3.028 × 10^3 g·m^{-3}), j is the sampling, $C(i)_j$ is the concentration of the element i in the j^{th} sampling (g·m^{-3}), Q is the solution flow rate (m^3·s^{-1}), SSA is the specific surface area of powder sample (m^2·g^{-1}), m is the mass of glass (g), x_i is the weight fraction of element i in the glass, and $t_{j+1} - t_j$ is the time between two samplings (s).

Alteration in static conditions was measured in perfluoroalkoxy reactors (PFA) at 22, 40, and 70 °C in 4% (v/v) acetic acid solution and in 4% (v/v) acetic acid solution initially saturated with respect to amorphous silica (170 mg·L^{-1}). The mass of glass powder (20−40 μm and 63−125 μm particle size fractions) was adjusted to have the desired glass-surface-area-to-solution-volume ratios (SA/V). The samplings were acidified by HNO_3 and analyzed by ICP-OES. The equivalent thicknesses of altered glass, Eth_i (m), were calculated with eq 2

$$Eth_i(t) = \frac{1}{\rho}\left[Eth_i(t-1) + \frac{(C(i)_t - C(i)_{t-1}) \times V_t}{\rho \times SSA \times m \times x_i}\right] \quad (2)$$

where $C(i)_t$ is the concentration of the element i in solution at time t, V_t is the volume of solution sampling at time t, and ρ is the glass density.

The glass forward dissolution rate r_0 is given by

DOI: 10.1021/acs.est.6b02971
Environ. Sci. Technol. 2016, 50, 11549−11558

Table 1. ^{17}O NMR Parameters Obtained by Fitting the ^{17}O MAS NMR Data of Pristine and Altered Glass (Standard Deviations, Depending on the Distribution of Each Parameter, Are Indicated in Parentheses) Using As Constraints the Parameters Extracted from the ^{17}O MQMAS NMR Data[a]

				proportion from	
	site	^{17}O NMR parameters		composition	^{17}O NMR
pristine glass	Si−O−Si	δ_{iso} (ppm) − ($\sigma_{\delta_{iso}}$)	52.5 (7.3)	78%	78%
		C_Q (MHz) − (σ_{C_Q})	4.8 (0.3)		
		η_Q − (σ_{η_Q})	0.3 (0.1)		
	Si−O−(Pb,K)	δ_{iso} (ppm) − ($\sigma_{\delta_{iso}}$)	118.7 (10.8)	9% (Si−O−Pb)	14%
		C_Q (MHz) − (σ_{C_Q})	3.1 (0.5)		
		η_Q − (σ_{η_Q})	0.6 (0.2)		
	Si−O−K	δ_{iso} (ppm) − ($\sigma_{\delta_{iso}}$)	74.8 (9.2)	13%	8%
		C_Q (MHz) − (σ_{C_Q})	2.2 (0.5)		
		η_Q − (σ_{η_Q})	0.6 (0.2)		
altered glass	Si−O−Si	δ_{iso} (ppm) − ($\sigma_{\delta_{iso}}$)	42.0 (5.0)	89%	89%
		C_Q (MHz) − (σ_{C_Q})	5.2 (0.2)		
		η_Q − (σ_{η_Q})	0.2 (0.1)		
	Si−O−(Pb,K)	δ_{iso} (ppm) − ($\sigma_{\delta_{iso}}$)	130.0 (12.0)	8% (Si−O−Pb)	6%
		C_Q (MHz) − (σ_{C_Q})	3.1 (0.5)		
		η_Q − (σ_{η_Q})	0.6 (0.2)		
	Si−O−K	δ_{iso} (ppm) − ($\sigma_{\delta_{iso}}$)	74.8 (9.2)	3%	1%
		C_Q (MHz) − (σ_{C_Q})	2.2 (0.5)		
		η_Q − (σ_{η_Q})	0.6 (0.2)		
	Si−O−H	δ_{iso} (ppm) − ($\sigma_{\delta_{iso}}$)	15.3 (1.9)		4%
		C_Q (MHz) − (σ_{C_Q})	3.7 (0.2)		
		η_Q − (σ_{η_Q})	0.4 (0.3)		

[a]The C_Q precision is 0.25 MHz and δ_{iso} precision is 2 ppm. The site proportions calculated from the composition of pristine and altered glasses are compared with the ^{17}O NMR quantification.

$$r_0(t) = \frac{d(Eth_{Si})}{dt} \quad (3)$$

where Eth_{Si} is the equivalent thickness of altered glass from Si dissolution.

III. RESULTS AND DISCUSSION

1. Pristine Lead Crystal Glass Structure. *^{29}Si MAS NMR.* Two contributions were observed at −94 ppm and −106 ppm on the ^{29}Si MAS NMR spectrum for pristine glass (Figure 1a), which correspond to the Q^3 and Q^4 entities, respectively, in agreement with the data obtained on lead silica binary glasses.[39,40] The simulation of the ^{29}Si spectra gave a proportion of 59% of Q^3 and 41% of Q^4 units (see Supporting Information, Figure S1). The resulting number of NBOs is then 25.7%. The calculation of the NBOs based on the glass composition, considering that two NBOs are formed from Na_2O, K_2O, and PbO (without postulating free oxygen atoms), leads to a value of 25.6%, very close to the experimental value.

^{17}O MAS NMR. The ^{17}O MAS NMR spectrum of the pristine glass (Figure 1b) enables three contributions to be resolved. A wide line at the −20 to 50 ppm range with a characteristic second-order quadrupolar line shape corresponds to the bridging oxygens Si−O−Si. Two narrower featureless peaks centered on 70 and 110 ppm are related to the NBOs and may be attributed to Si−O−K and Si−O−(Pb,K), respectively (the latter corresponds to regions where Pb and K are mixed around the NBOs). This attribution will be discussed hereafter from the MQMAS NMR data.

^{17}O MQMAS NMR. The three contributions related to Si, K, and Pb are clearly separated on the experimental and simulated ^{17}O MQMAS spectra shown in Figure 2(a,b). The simulated spectrum, generated using a 3D distribution of the NMR parameters (taking into account the correlation effects between these parameters[38]), shows very good agreement with the experimental spectrum. Figure 2c shows the two-dimensional projection of the distribution of the NMR parameters, the isotropic chemical shift (δ_{iso}), and the quadrupolar coupling constant (C_Q), extracted from the MQMAS NMR spectrum. Lee and Kim[24] recently reported the structural evolution of binary lead silicate glasses from ^{17}O MQMAS NMR for high PbO contents close to the orthosilicate composition ranging from 60 mol % to 71 mol %. They clearly pointed out the presence Pb−O−Pb bonds which increase with Pb content at the expense of Si−O−Si bonds. The authors represented Pb and Si mixing sites in the form $^{[n]}Pb-^{[m]}O-^{[4]}Si$, where n = 3, 4 and m = 2, 3, 4. Under these conditions, the same oxygen atom could be involved in both Pb−O−Si and Pb−O−Pb bonds. The absence of Pb−O−Pb contribution (within the NMR detection limit) in our crystal glass suggests that Pb structural configuration may be fairly close to that of an alkaline-earth type network modifier. The positions of Si−O−Pb and Pb−O−Pb obtained by Lee and Kim[24] are reported on our ^{17}O MQMAS NMR spectrum in Supporting Information (Figure S2).

Furthermore, the nature of the alkali cation at the origin of the NBO formation modifies the position of the ^{17}O line; a sodium disilicate decreases the NBO δ_{iso} by about 40 ppm

DOI: 10.1021/acs.est.6b02971
Environ. Sci. Technol. 2016, 50, 11549−11558

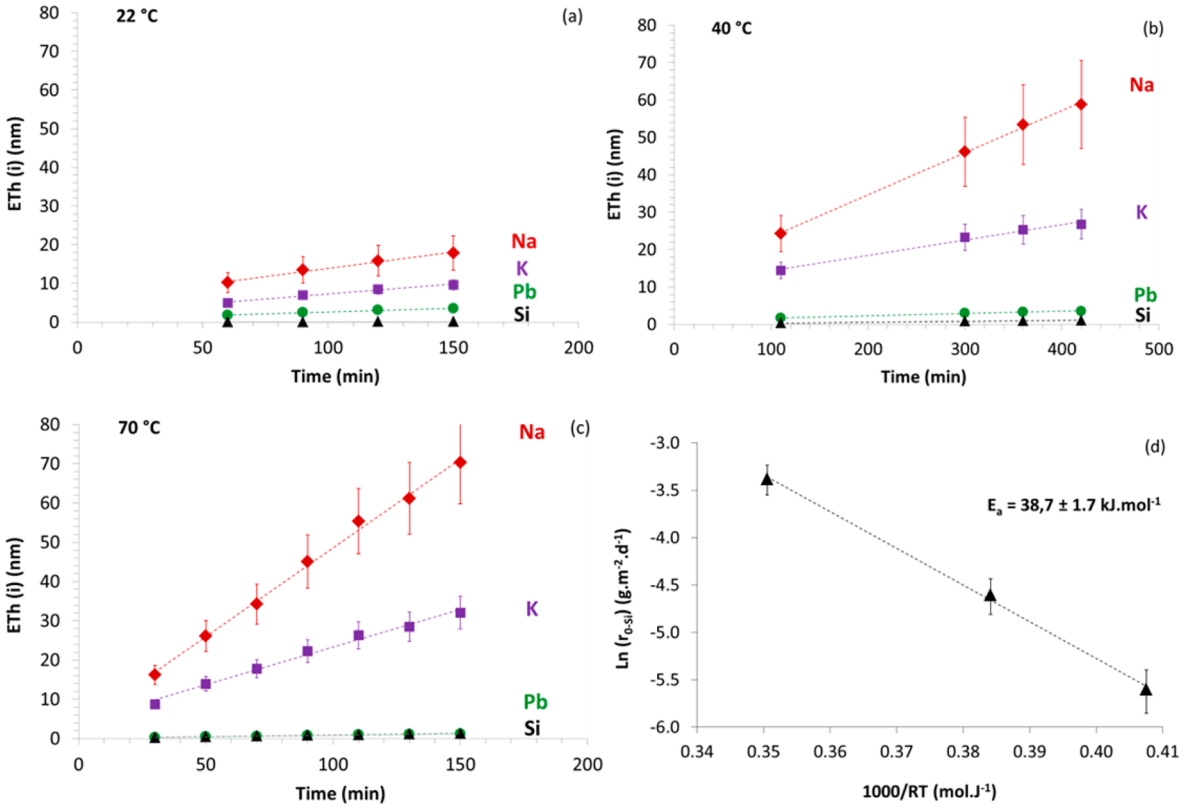

Figure 3. Equivalent thicknesses of altered glass calculated from the release of Si, Pb, K, and Na at 22 °C (a), 40 °C (b), and 70 °C (c) into acetic acid solution, in forward dissolution rate regime. Broken lines are simple visual aids. (d) Determination of the apparent activation energy E_a for the alteration mechanisms in forward dissolution rate regime r_0 (from the release of Si, eq 3).

compared to a potassium disilicate.[41] The position of the NBO site at around 75 ppm (Figure 2c) can be attributed here to Si−O−K, Si−O−Na being expected at around 40 ppm.[38] Given the low Na content in the glass (below one percent) and the sensitivity of the MQMAS experiment, it remains challenging to observe Si−O−Na contribution on the ^{17}O MQMAS NMR spectrum.

Some previous works carried out on binary sodium silicate glasses with SiO_2 content close to that studied here reported ^{17}O NMR parameters for the Si−O−Si site similar to those obtained for our crystal glass.[38,42] Under these conditions, the addition of Pb to the glass does not seem to have a major effect on the Si−O−Si site geometry, either for the angular distributions (which influence the quadrupolar parameters[42−44]) or the Si−O bond distances (which influence the isotropic chemical shift[45,46]). In the binary lead silicate glasses studied by Lee and Kim,[24] the Si−O−Pb δ_{iso} was located at around 151 ppm, and it slightly increased with Pb content. For our glass composition, the contribution related to Pb is close to 119 ppm (see Table 1). The quantification of the three oxygen sites enables the origin of this difference to be discussed.

By first assuming that the three ^{17}O contributions revealed by the MQMAS NMR spectrum can be attributed to Si−O−Si, Si−O−Pb, and Si−O−K, Table 1 compares their proportions calculated from the crystal glass chemical composition and those obtained from the NMR quantification. It clearly appears that the quantity of Si−O−Pb (14%) is higher than expected from the composition (8.7%), unlike for Si−O−K where the quantity is lower (8% experimentally instead of the expected 12.7%). This observation highlights that Si−O−Pb contribution does not only contain Pb and Si cations but also rather a mixing of Pb and K, noted as Si−O−(Pb,K), as had been previously observed for other types of cations.[47−49] Following the NMR quantification, Si−O−(Pb,K) would be constituted of 38% of K and 62% of Pb. This effect thus explains the lower ^{17}O δ_{iso} of the Pb site in the glass studied here compared to the binary glasses[24] (Supporting Information, Figure S2); the Si−O−(Pb,K) site at 119 ppm is situated between Si−O−K at 75 ppm and Si−O−Pb at 151 ppm. Finally, it should be noted that the wider distribution of ^{17}O δ_{iso} for Si−O−(Pb,K) (Figure 2c) is probably the result of a greater chemical disorder for the Pb−K dissimilar pair.

It is worth noting that by taking into account the difference in chemical shift between Si−O−Pb at 151 ppm and Si−O−K at 75 ppm, weighting of the value obtained for Si−O−(Pb,K) at 119 ppm would give a K quantity of 42%, very close to the value directly deduced from the NMR quantification (38%). It therefore appears that ^{17}O δ_{iso} of Si−O−(Pb,K) could provide information regarding the proportion of K mixing with Pb in the NBO environment.

2. Lead Crystal Glass Leaching. For the first set of experiments, the most favorable conditions for accessing silicate network hydrolysis mechanisms were performed, based on a high renewal rate of a 4% (v/v) acetic acid solution. Figures 3(a,b,c) show the equivalent alteration thicknesses of Na, K, Pb, and Si at 22, 40, and 70 °C calculated from eq 1. The leaching of Sb (not shown) was very close to Si. Activation energy for hydrolysis mechanisms in the forward dissolution rate regime, based on an Arrhenius law, is given from the Si dissolution rate (Figure 3d). The linearity between the three temperatures points out the good agreement of the data, resulting in an activation energy of 38.7 ± 1.7 kJ mol^{-1}. It can be concluded

DOI: 10.1021/acs.est.6b02971
Environ. Sci. Technol. 2016, 50, 11549−11558

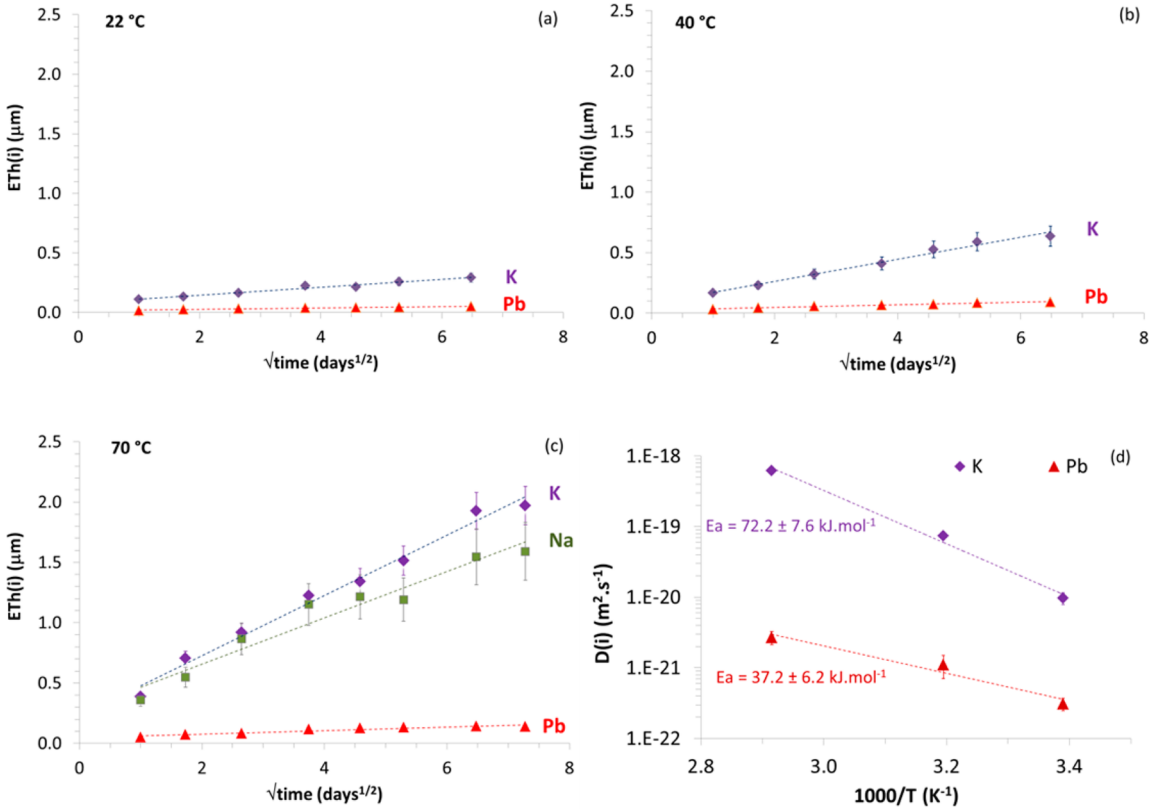

Figure 4. Equivalent thicknesses of altered glass calculated from the release of Pb, K, and Na at 22 °C (a), 40 °C (b), and 70 °C (c) into acetic acid solution, in a solution initially saturated with respect to amorphous silica (SA/V = 100 m^{-1}). Broken lines are simple visual aids. (d) Representation of the diffusion coefficients as a function of the reciprocal of the temperature. The activation energy E_a is given by the slope of the lines.

that within the temperature range studied (22−70 °C), the dissolution of the silicate network is controlled by the same mechanisms. The low value of activation energy suggests that the dissolution of Si is due not only to reaction surface control by hydrolysis but also to transport control by interdiffusion.[50]

The dissolution was significantly noncongruent; while the release of Pb and Sb were fairly close to the Si network former, K and Na were released much more rapidly. It is tricky to calculate unique activation energy for Pb, K, and Na as the nonlinearity observed between the three temperatures strongly suggests that the leaching of Pb, K, and Na resulted from various mechanisms. At 22 °C, an interdiffusion mechanism may probably be favored, whereas at 70 °C network hydrolysis may be prevalent.[51]

For the second set of experiments, a solution initially saturated with respect to amorphous silica was used in order to specifically focus on the interdiffusion mechanisms,[32] with a SA/V ratio of 100 m^{-1}. It has recently been shown that there was no hydrolysis of Si under these conditions.[32] Figure 4(a,b,c) compares the equivalent alteration thicknesses of K and Pb at 22, 40, and 70 °C as a function of the square root of time. The very low concentration of Na in the glass (0.8 mol %) made its measurement in solution only possible at 70 °C. It was then observed that it behaved like K. Analogous behavior of Na and K may therefore be expected at lower temperatures.

The resulting linear behavior with respect to square root of time suggests that the different cations are released in solution by a diffusive mechanism. The leaching of Pb was much lower than K. The Pb behavior thus seems to be assimilated with multivalent elements, like the alkaline earths or the rare earth elements, which are leached much more slowly than the alkalis.[48] Fick's second law was used to derive the apparent diffusion coefficients at the interface between the glass and the solution by fitting the curves in Figures 4(a,b,c). The concentration in solution is then given by[52]

$$C(i) = 2\frac{\mathrm{SSA} \times m}{V} C_{gi}\left(\frac{D_i \times t}{\pi}\right)^{1/2} \quad (4)$$

where $C(i)$ is the concentration of element i (i = Pb or K) in solution, C_{gi} is the concentration of Pb or K in the glass, V is the volume of the solution, and D_i is the diffusion coefficient for Pb or K.

Figure 4d shows the evolution of the diffusion coefficients as a function of the temperature for Pb and K. The resulting activation energies highlight a temperature dependence which is much lower for Pb than for K, with values of 37.2 ± 6.2 kJ·mol^{-1} and 72.2 ± 7.6 kJ·mol^{-1}, respectively. At 22 °C, a low diffusion coefficient of (3.1 ± 0.6)·10^{-22} m^2·s^{-1} is determined for Pb. Depending on the temperature, Pb diffusion into solution is between 1 and 2 orders of magnitude slower than the alkalis.

For higher Pb contents, from 25 to 70 mol %, diffusion coefficients of more than 4 orders of magnitude higher were obtained in glasses altered in 0.1 or 0.5 N HNO_3 solutions.[8,10] A percolation mechanism through the plumbate subnetwork was observed at 40 °C.[10] Binary lead silicate glasses with PbO starting from an approximately 33 mol % content had a diffusion coefficient increasing by about 1 order of magnitude when PbO content increased by 5%.[10] One single composition was studied at a lower Pb content (25 mol %) below the percolation threshold; at about 10^{-17} m^2·s^{-1}, it showed less

DOI: 10.1021/acs.est.6b02971
Environ. Sci. Technol. 2016, 50, 11549−11558

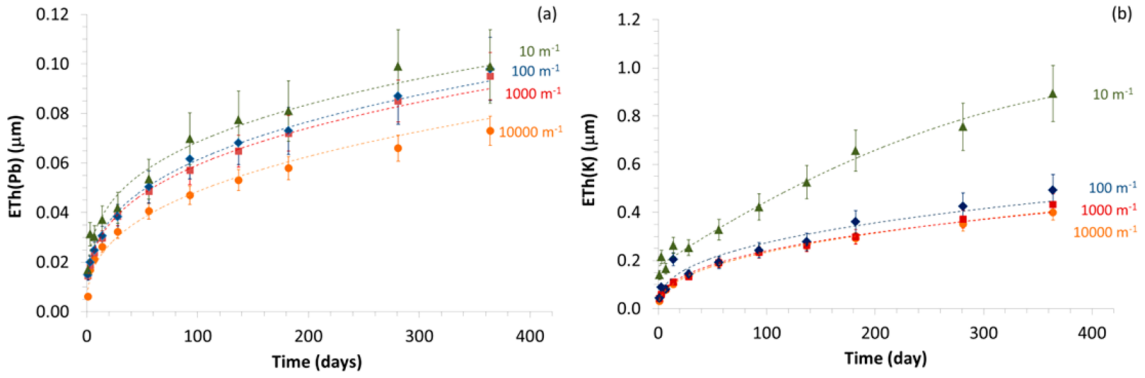

Figure 5. Equivalent thicknesses of altered glass calculated from the release of (a) Pb and (b) K at 22 °C into acetic acid solution for different SA/*V* ratios (10, 100, 1000, and 10000 m^{-1}). Broken lines are simple visual aids.

pronounced diffusion coefficient variations, suggesting a plateau. If this latter value is not taken into account, so if the data located within the percolation regime are extrapolated from our glass composition containing 10.6 mol % of PbO, a similar value (10^{-22} $m^2 \cdot s^{-1}$) close to that found in our study (10^{-21} $m^2 \cdot s^{-1}$) is obtained. This value is far away from the plateau which was observed at 10^{-17} $m^2 \cdot s^{-1}$ for 25 mol % of PbO (see Supporting Information, Figure S3). Then, the sharp drop in the diffusion coefficient could be due to a second percolation threshold, which would explain the high difference between 10 and 25 mol % of PbO. The early formation of Pb−O−Pb bonds with the increase in the Pb concentration, even if they do not yet constitute a plumbate subnetwork, could lead to this second percolation threshold beyond which an increase in Pb release kinetics would occur.

Finally, in order to reach more advanced reaction progress, a third set of experiments was carried out in static conditions at different SA/*V* ratios, varying from 10 m^{-1} to 10000 m^{-1}. These long-term experiments were conducted at 22 °C in 4% acetic acid solution (without Si in the initial solution), for one year. Although there were 3 orders of magnitude between the surface to volume ratios, Figure 5 reports small variations in the leaching of Pb and K, showing that their releases remain controlled by interdiffusion, a mechanism that is not surface dependent. As expected from our previous experiments, Pb leaching is much lower than K. The calculation of the retention factor RF for Pb compared to K ($RF_{(Pb)} = 1 - Eth(Pb)/Eth(K)$) for the various SA/*V* ratios gave similar values, with an average retention of 77% of Pb in the alteration layer. It may be noted that Pb concentrations in solution always remain much lower (by at least 3 orders of magnitude) than the solubility of lead acetate.[53] This confirms that the release of Pb is not controlled by its solubility limit but by diffusion mechanisms.

From the Pb diffusion coefficients given by the interdiffusion experiments (Figure 4d), an equation using the formalism of eq 4 was obtained to calculate the Pb concentration in acetic acid solution, as a function of the SA/*V* ratio, the temperature, and the leaching time (eq 5). This equation gives good agreement with the experimental data (see Supporting Information, Figure S4). It can be applied in the range of temperature studied (22 °C−70 °C) for time periods during which the Pb leaching remains controlled by diffusion mechanisms

$$C_{Pb} = 3.4 \cdot 10^{-2} \times \frac{S}{V} \times (e^{-E_a/RT} \times t)^{1/2} \quad (5)$$

where C_{Pb} is the concentration of lead in solution ($mg \cdot L^{-1}$), *t* is the time of alteration (s), *V* is the volume of the solution (m^3), *S* is the surface of the glass (m^2), *T* is the temperature (K), E_a is the activation energy of the lead diffusion (37200 $J \cdot mol^{-1}$), and *R* is the gas constant (8.31 $J \cdot mol^{-1} \cdot K^{-1}$).

It is worth noting that the diffusion coefficients were measured in an acetic acid solution having a pH of 2.3. An increase of the pH is expected to decrease the diffusion coefficient.[51] In our 1 year experiments, the pH was stable, except for the higher *SA*/V ratio (10000 m^{-1}) for which the pH reached 3.3. This higher pH value may reflect that the experimental Pb concentrations are slightly lower than the calculated values (Supporting Information, Figure S4). Eq 5 may be used to obtain an order of magnitude of Pb concentrations depending on the geometry of materials and their conditions of use.

3. Alteration Layer Characterization. *Elemental Profiles.* Figure 6 displays the elemental profiles obtained by ToF-SIMS on the glass altered at 70 °C in acetic acid solution saturated with respect to amorphous silica after 1, 7, and 53 days. The progress of the alteration front is clearly visible over time. At the interface between the pristine glass and the alteration layer, the hydration front can be seen progressing, with a greater penetration of hydrogen compared to the alkalis depletion. The profiles for Na and K are very similar, in agreement with the concentrations measured in solution (Figure 4c). Pb was clearly released to a lesser extent than the alkalis and is only depleted on a thin external surface of the alteration layer. After 53 days, the depth of Pb depletion was 15 times less than the total thickness of the alteration layer. The equivalent thicknesses for the solution analyses are in quite good agreement with the depths obtained from the ToF-SIMS profiles. The small differences remaining between the two methods could be explained because (i) calculation of Eth using the SSA of glass powder measured by BET underestimates Eth[54] (ii) a part of K (~20−30%) is retained in the alteration layer and therefore not released into solution and (iii) there may exist variations in the abrasion rate of ToF-SIMS between the alteration layer external surface and the pristine glass, because of potentially different densities.

The elemental profiles obtained after one year of alteration at various SA/*V* ratios at 22 °C were very similar than the profiles obtained at 70 °C for shorter periods. In particular, the three areas remain still observed: the hydration front, the alkalis depletion, and the Pb-depleted external surface which is still maintained for long-term experiments (see Supporting Information, Figure S5). Unlike the experiments at 70 °C, the experiments at 22 °C were conducted in acetic acid solution without saturation with respect to amorphous silica. In the first

DOI: 10.1021/acs.est.6b02971
Environ. Sci. Technol. 2016, 50, 11549−11558

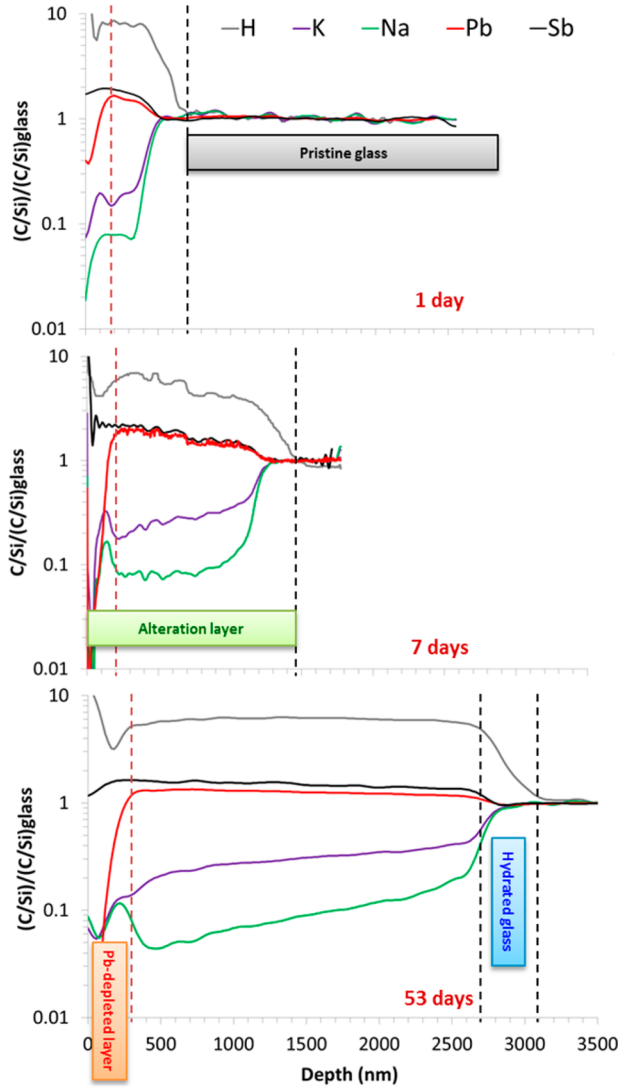

Figure 6. Elemental profiles obtained by ToF-SIMS on the glass altered at 70 °C for 1, 7, and 53 days in acetic acid solution saturated with respect to amorphous silica (SA/V = 100 m^{-1}). Data have been normalized compared to Si, which is the least soluble element. All the elements are thus normalized to 1 in the pristine glass; data lower than 1 indicate a depletion of the element, whereas data higher than 1 indicate an enrichment.

case, the Pb release is then only controlled by diffusion mechanisms. In both cases, however, the elemental profiles were very similar, indicating the limited influence of hydrolysis on the Pb release.

Altered Lead Crystal Glass Structure. Small glass powders of a few microns were entirely altered under static conditions at 70 °C in a 4% acetic acid solution containing oxygen-17 enriched water, in order to specifically probe the alteration layer by ^{17}O NMR. An experiment in oxygen-16 carried out in parallel and under the same SA/V ratio, but with a greater volume of solution, enabled the concentrations of elements in solution to be measured. This allowed the experiment to be stopped when all the glass had been altered, based on the release of Na in solution, and to estimate the alteration layer molar composition deduced from the solution analysis: $88.7SiO_2 - 2.5K_2O - 7.9PbO - 1.0Sb_2O_3$.

Figure 1a compares the ^{29}Si MAS NMR spectra for the pristine commercial lead crystal glass and for the same glass altered in oxygen-17 enriched solution. An obvious reorganization within the alteration layer through a silicate network polymerization is clearly highlighted, as usually observed in silicate glasses.[55−57] Centered on the Q^2-Q^3 species in the pristine glass, a majority of the Si forms Q^4 units in the alteration layer. Quantification of the NBOs was carried out based on the ^{17}O NMR data of Figure 1b (reported in Table 1). The ^{17}O MAS NMR spectrum of altered glass clearly confirms that most of K had been released into solution, whereas a significant part of Pb remained in the alteration layer. The Si−O−(Pb,K) line is shifted toward the higher chemical shifts. Its position becomes closer to the Si−O−Pb contribution observed in binary lead silicate glasses,[24] indicating a lower level of mixing between Pb and K. This shows that K is preferentially extracted compared to Pb in mixed Si−O−(Pb,K).

The pristine glass composition ($77.1SiO_2 - 0.8Na_2O - 11.3K_2O - 10.6PbO - 0.2Sb_2O_3$) can be compared with the altered glass obtained by the mass balance from the solution analysis ($88.7SiO_2 - 2.5K_2O - 7.9PbO - 1.0Sb_2O_3$). It should however be noted that the NMR indicates a higher SiO_2 content (93% instead of 89%). This is related to the presence of Si−OH sites which overlay the Si−O−Si contribution on the spectrum.[58] ^1H MAS NMR spectra enabled to resolve the proton speciation, with molecular water and two Si−OH depending on the strength of their hydrogen bonding (see Supporting Information, Figure S6). The Si−OH contributions were more clearly revealed from 2D heteronuclear correlation maps ($^1H \rightarrow {}^{17}O$ HETCOR) (see Supporting Information, Figure S7). The NMR parameters considered for this site (Table 1) come from the work of Brunet et al.[58] From these data, simulation of the ^{17}O MAS spectrum gave 4% of Si−OH sites (see Supporting Information, Figure S7b). The total number of NBOs of 11% is quite comparable to the NBOs deduced from the alteration layer composition (10.9%). The repolymerization led to a decrease in the NBOs, dropping from 26% in the pristine glass to 11% in the alteration layer. A significant decrease can be noted for the width of the NMR parameter distribution for Si−O−Si (related to higher Si−O−Si mean bond angles), as well as an increase in the quadrupolar coupling constant, closer to that in vitreous silicon[59] (Table 1). These findings highlight the reorganization of the polymerized silicate network.

The behavior of Pb is closely related to the structural configuration it adopts, as much in the pristine glass as in the alteration layer. Homogeneously dispersed within the silicate network, the leaching of Pb is less favorable, and its release into solution is lower than the alkalis. When present at a higher concentration than in the crystal glass studied here, Pb may form clusters, and its leaching increases, probably as soon as it forms Pb−O−Pb bonds. For 45 wt % of PbO in a glass containing Na and K, it has been reported that the alkalis and Pb were released at the same rate.[11] At higher concentration, there is a percolation of the Pb subnetwork, which is preferentially highly released into solution. These high Pb contents seem to give rise to a surface enrichment in Pb.[11,12] No such enrichment was observed for our crystal glass; conversely, Pb is depleted in the outermost part of the alteration layer. In the remaining part, it stays surrounded by Si in a stable structural configuration similar to that of the pristine glass.

The data obtained from this work enabled parameters to be set for a simple predictive mechanistic model for lead leaching

DOI: 10.1021/acs.est.6b02971
Environ. Sci. Technol. 2016, 50, 11549−11558

from commercial crystal glass during diffusion-controlled dissolution in acetic acid solution.

■ ASSOCIATED CONTENT

Supporting Information

The Supporting Information is available free of charge on the ACS Publications website at DOI: 10.1021/acs.est.6b02971.

Figures S1−S7 (PDF)

■ AUTHOR INFORMATION

Corresponding Author

*E-mail: frederic.angeli@cea.fr.

Notes

The authors declare no competing financial interest.

■ REFERENCES

(1) Szaloki, I.; Braun, M.; Van Grieken, R. Quantitative characterisation of the leaching of lead and other elements from glazed surfaces of historical ceramics. *J. Anal. At. Spectrom.* **2000**, *15* (7), 843−850.

(2) Cohen, B. M.; Uhlmann, D. R.; Shaw, R. R. Optical and electrical properties of lead silicate glasses. *J. Non-Cryst. Solids* **1973**, *12* (2), 177−188.

(3) Barker, R. S.; McConkey, E. A.; Richards, D. Effect of Gamma Radiation on Optical Absorption of Lead Silicate Glass. *Phys. Chem. Glasses* **1965**, *6* (1), 24.

(4) Patrick, L. Lead toxicity, a review of the literature. Part 1: Exposure, evaluation, and treatment. *Altern. Med. Rev.* **2006**, *11* (1), 2−22.

(5) Graziano, J. H.; Blum, C. B.; Lolacono, N. J.; Slavkovich, V.; Manton, W. I.; Pond, S.; Moore, M. R. Human in vivo model for the determination of lead bioavailability using stable isotope dilution. *Environ. Health Perspect.* **1996**, *104* (2), 176−179.

(6) van Elteren, J. T.; Grilc, M.; Beeston, M. P.; Reig, M. S.; Grgic, I. An integrated experimental-modeling approach to study the acid leaching behavior of lead from sub-micrometer lead silicate glass particles. *J. Hazard. Mater.* **2013**, *262*, 240−249.

(7) Rahimi, R. A.; Sadrnezhaad, S. K. Effects of Ion-Exchange and Hydrolysis Mechanisms on Lead Silicate Glass Corrosion. *Corrosion* **2012**, *68* (9), 793−800.

(8) Rahimi, R. A.; Sadrnezhaad, S. K.; Raisali, G.; Hamidi, A. Hydrolysis kinetics of lead silicate glass in acid solution. *J. Nucl. Mater.* **2009**, *389* (3), 427−431.

(9) Sadrnezhaad, S. K.; Rahimi, R. A.; Raisali, G.; Foruzanfar, F. Mechanism of deleading of silicate glass by 0.5 N HNO3. *J. Non-Cryst. Solids* **2009**, *355* (48−49), 2400−2404.

(10) Mizuno, M.; Takahashi, M.; Takaishi, T.; Yoko, T. Leaching of lead and connectivity of plumbate networks in lead silicate glasses. *J. Am. Ceram. Soc.* **2005**, *88* (10), 2908−2912.

(11) Bertoncello, R.; Milanese, L.; Bouquillon, A.; Dran, J. C.; Mille, B.; Salomon, J. Leaching of lead silicate glasses in acid environment: compositional and structural changes. *Appl. Phys. A: Mater. Sci. Process.* **2004**, *79* (2), 193−198.

(12) Bonnet, C.; Bouquillon, A.; Turrell, S.; Deram, V.; Mille, B.; Salomon, J.; Thomassin, J. H.; Fiaud, C. Alteration of lead silicate glasses due to leaching in heated acid solutions. *J. Non-Cryst. Solids* **2003**, *323* (1−3), 214−220.

(13) Guadagnino, E.; Gambaro, M.; Gramiccioni, L.; Denaro, M.; Feliciani, R.; Baldini, M.; Stacchini, P.; Giovannangeli, S.; Carelli, G.; Castellino, N.; Vinci, F. Estimation of lead intake from crystalware under conditions of consumer use. *Food Addit. Contam.* **2000**, *17* (3), 205−218.

(14) Guadagnino, E.; Verita, M.; Geotti-Bianchini, F.; Shallenberger, J.; Pantano, C. G. Surface analysis of 24% lead crystal glass articles: correlation with lead release. *Glass Technol.* **2002**, *43* (2), 63−69.

(15) Schultz-Munzenberg, C.; Meisel, W.; Gutlich, P. Changes of lead silicate glasses induced by leaching. *J. Non-Cryst. Solids* **1998**, *238* (1−2), 83−90.

(16) Ahmed, A. A.; Youssof, I. M. Effect of repeated leaching on the release of lead and other cations from lead crystal glass (24% PbO) by acid solutions and water. *Glass Technol.* **1997**, *38* (5), 171−178.

(17) Ahmed, A. A.; Youssof, I. M. Interaction between lead crystal glass (24% PbO) and acetic acid. *Glastech. Ber.-Glass Sci. Technol.* **1997**, *70* (6), 173−185.

(18) Ahmed, A. A.; Youssof, I. M. Reactions between water and lead crystal glass (24% PbO). *Glass Technol.* **1997**, *38* (1), 30−38.

(19) Cailleteau, C.; Weigel, C.; Ledieu, A.; Barboux, P.; Devreux, F. On the effect of glass composition in the dissolution of glasses by water. *J. Non-Cryst. Solids* **2008**, *354* (2−9), 117−123.

(20) Graziano, J. H.; Blum, C. Lead-Exposure from Lead Crystal. *Lancet* **1991**, *337* (8734), 141−142.

(21) Kanunnikova, O. M.; Goncharov, O. Y. X-ray photoelectron analysis of lead-silicate glass structure. *J. Appl. Spectrosc.* **2009**, *76* (2), 194−202.

(22) Wang, P. W.; Zhang, L. P. Structural role of lead in lead silicate glasses derived from XPS spectra. *J. Non-Cryst. Solids* **1996**, *194* (1−2), 129−134.

(23) Alderman, O. L. G.; Hannon, A. C.; Holland, D.; Feller, S.; Lehr, G.; Vitale, A. J.; Hoppe, U.; von Zimmerman, M.; Watenphul, A. Lone-pair distribution and plumbite network formation in high lead silicate glass, 80PbO center dot 20SiO(2). *Phys. Chem. Chem. Phys.* **2013**, *15* (22), 8506−8519.

(24) Lee, S. K.; Kim, E. J. Probing Metal-Bridging Oxygen and Configurational Disorder in Amorphous Lead Silicates: Insights from O-17 Solid-State Nuclear Magnetic Resonance. *J. Phys. Chem. C* **2015**, *119* (1), 748−756.

(25) Dalby, K. N.; Nesbitt, H. W.; Zakaznova-Herzog, V. P.; King, P. L. Resolution of bridging oxygen signals from O 1s spectra of silicate glasses using XPS: Implications for O and Si speciation. *Geochim. Cosmochim. Acta* **2007**, *71* (17), 4297−4313.

(26) Takaishi, T.; Takahashi, M.; Jin, J.; Uchino, T.; Yoko, T.; Takahashi, M. Structural study on PbO-SiO2 glasses by X-ray and neutron diffraction and Si-29 MAS NMR measurements. *J. Am. Ceram. Soc.* **2005**, *88* (6), 1591−1596.

(27) Gee, I. A.; Holland, D.; McConville, C. F. Atomic environments in binary lead silicate and ternary alkali lead silicate glasses. *Phys. Chem. Glasses* **2001**, *42* (6), 339−348.

(28) Fayon, F.; Landron, C.; Sakurai, K.; Bessada, C.; Massiot, D. Pb2+ environment in lead silicate glasses probed by Pb-L-III edge XAFS and Pb-207 NMR. *J. Non-Cryst. Solids* **1999**, *243* (1), 39−44.

(29) Feller, S.; Lodden, G.; Riley, A.; Edwards, T.; Croskrey, J.; Schue, A.; Liss, D.; Stentz, D.; Blair, S.; Kelley, M.; Smith, G.; Singleton, S.; Affatigato, M.; Holland, D.; Smith, M. E.; Kamitsos, E. I.; Varsamis, C. P. E.; Ioannou, E. A multispectroscopic structural study of lead silicate glasses over an extended range of compositions. *J. Non-Cryst. Solids* **2010**, *356* (6−8), 304−313.

(30) Fajans, K.; Kreidl, N. J. Stability of Lead Glasses and Polarization of Ions. *J. Am. Ceram. Soc.* **1948**, *31* (4), 105−114.

(31) Carmona, N.; Garcia-Heras, M.; Gil, C.; Villegas, M. A. Chemical degradation of glasses under simulated marine medium. *Mater. Chem. Phys.* **2005**, *94* (1), 92−102.

(32) Gin, S.; Jollivet, P.; Fournier, M.; Angeli, F.; Frugier, P.; Charpentier, T. Origin and consequences of silicate glass passivation by surface layers. *Nat. Commun.* **2015**, *6*, 6360.

(33) Hight, S. C. Lead migration from lead crystal wine glasses. *Food Addit. Contam.* **1996**, *13* (7), 747−765.

(34) Angeli, F.; Charpentier, T.; Gaillard, M.; Jollivet, P. Influence of zirconium on the structure of pristine and leached soda-lime borosilicate glasses: Towards a quantitative approach by O-17 MQMAS NMR. *J. Non-Cryst. Solids* **2008**, *354* (31), 3713−3722.

(35) Larsen, F. H.; Farnan, I. Si-29 and O-17 (Q)CPMG-MAS solid-state NMR experiments as an optimum approach for half-integer nuclei having long T-1 relaxation times. *Chem. Phys. Lett.* **2002**, *357* (5−6), 403−408.

DOI: 10.1021/acs.est.6b02971
Environ. Sci. Technol. 2016, 50, 11549−11558

(36) Amoureux, J. P.; Fernandez, C.; Steuernagel, S. Z filtering in MQMAS NMR. *J. Magn. Reson., Ser. A* **1996**, *123* (1), 116−118.
(37) Fernandez, C.; Amoureux, J. P. 2D Multiquantum MAS-NMR Spectroscopy of AL-27 in Aluminophosphate Molecular-Sieves. *Chem. Phys. Lett.* **1995**, *242* (4−5), 449−454.
(38) Angeli, F.; Villain, O.; Schuller, S.; Ispas, S.; Charpentier, T. Insight into sodium silicate glass structural organization by multinuclear NMR combined with first-principles calculations. *Geochim. Cosmochim. Acta* **2011**, *75* (9), 2453−2469.
(39) Fayon, F.; Bessada, C.; Massiot, D.; Farnan, I.; Coutures, J. P. Si-29 and Pb-207 NMR study of local order in lead silicate glasses. *J. Non-Cryst. Solids* **1998**, *232-234*, 403−408.
(40) Shrikhande, V. K.; Sudarsan, V.; Kothiyal, G. P.; Kulshreshtha, S. K. Si-29 MAS NMR and microhardness studies of some lead silicate glasses with and without modifiers. *J. Non-Cryst. Solids* **2001**, *283* (1−3), 18−26.
(41) Florian, P.; Vermillion, K. E.; Grandinetti, P. J.; Farnan, I.; Stebbins, J. F. Cation distribution in mixed alkali disilicate glasses. *J. Am. Chem. Soc.* **1996**, *118* (14), 3493−3497.
(42) Lee, S. K.; Stebbins, J. F. Effects of the degree of polymerization on the structure of sodium silicate and aluminosilicate glasses and melts: An O-17 NMR study. *Geochim. Cosmochim. Acta* **2009**, *73* (4), 1109−1119.
(43) Clark, T. M.; Grandinetti, P. J. Calculation of bridging oxygen O-17 quadrupolar coupling parameters in alkali silicates: A combined ab initio investigation. *Solid State Nucl. Magn. Reson.* **2005**, *27* (4), 233−241.
(44) Clark, T. M.; Grandinetti, P. J.; Florian, P.; Stebbins, J. F. An O-17 NMR investigation of crystalline sodium metasilicate: Implications for the determination of local structure in alkali silicates. *J. Phys. Chem. B* **2001**, *105* (49), 12257−12265.
(45) Ashbrook, S. E.; Berry, A. J.; Wimperis, S. O-17 multiple-quantum MAS NMR study of high-pressure hydrous magnesium silicates. *J. Am. Chem. Soc.* **2001**, *123* (26), 6360−6366.
(46) Ashbrook, S. E.; Berry, A. J.; Wimperis, S. O-17 multiple-quantum MAS NMR study of pyroxenes. *J. Phys. Chem. B* **2002**, *106* (4), 773−778.
(47) Lee, S. K.; Stebbins, J. F. Nature of cation mixing and ordering in Na-Ca silicate glasses and melts. *J. Phys. Chem. B* **2003**, *107* (14), 3141−3148.
(48) Angeli, F.; Charpentier, T.; Molieres, E.; Soleilhavoup, A.; Jollivet, P.; Gin, S. Influence of lanthanum on borosilicate glass structure: A multinuclear MAS and MQMAS NMR investigation. *J. Non-Cryst. Solids* **2013**, *376*, 189−198.
(49) Lee, S. K.; Mysen, B. O.; Cody, G. D. Chemical order in mixed-cation silicate glasses and melts. *Phys. Rev. B: Condens. Matter Mater. Phys.* **2003**, *68* (21), 7.
(50) Guy, C.; Schott, J. Multisite Surface-Reaction versus Transport Control during the Hydrolysis of a Complex Oxide. *Chem. Geol.* **1989**, *78* (3−4), 181−204.
(51) Parruzot, B.; Jollivet, P.; Rebiscoul, D.; Gin, S. Long-term alteration of basaltic glass: Mechanisms and rates. *Geochim. Cosmochim. Acta* **2015**, *154*, 28−48.
(52) Helebrant, A.; Pekarkova, I. Kinetics of glass corrosion in acid solutions. *Ber. Bunsen-Ges. Phys. Chem. Chem. Phys.* **1996**, *100* (9), 1519−1522.
(53) Apelblat, A.; Manzurola, E. Solubilities of manganese, cadmium, mercury and lead acetates in water from T = 278.15 K to T = 340.15 K. *J. Chem. Thermodyn.* **2001**, *33* (2), 147−153.
(54) Fournier, M.; Ull, A.; Nicoleau, E.; Inagaki, Y.; Odorico, M.; Frugier, P.; Gin, S. Glass dissolution rate measurement and calculation revisited. *J. Nucl. Mater.* **2016**, *476*, 140−154.
(55) Bunker, B. C. Molecular Mechanisms for Corrosion of Silica and Silicate-Glasses. *J. Non-Cryst. Solids* **1994**, *179*, 300−308.
(56) Casey, W. H.; Westrich, H. R.; Banfield, J. F.; Ferruzzi, G.; Arnold, G. W. Leaching and Reconstruction at the Surfaces of Dissolving Chain-Silicate Minerals. *Nature* **1993**, *366* (6452), 253−256.
(57) Angeli, F.; Gaillard, M.; Jollivet, P.; Charpentier, T. Influence of glass composition and alteration solution on leached silicate glass structure: A solid-state NMR investigation. *Geochim. Cosmochim. Acta* **2006**, *70* (10), 2577−2590.
(58) Brunet, F.; Charpentier, T.; Le Caer, S.; Renault, J. P. Solid-state NMR characterization of a controlled-pore glass and of the effects of electron irradiation. *Solid State Nucl. Magn. Reson.* **2008**, *33* (1−2), 1−11.
(59) Charpentier, T.; Kroll, P.; Mauri, F. First-Principles Nuclear Magnetic Resonance Structural Analysis of Vitreous Silica. *J. Phys. Chem. C* **2009**, *113* (18), 7917−7929.

NOTE ADDED AFTER ASAP PUBLICATION

This paper was published ASAP on October 21, 2016 with incomplete figure captions for Figure 3 and Figure 4. The corrected version was reposted to the Web on October 24, 2016.

DOI: 10.1021/acs.est.6b02971
Environ. Sci. Technol. 2016, 50, 11549−11558